Cardiovascular Diabetology

RESEARCH

Open Access

Cellular crosstalk in organotypic vasculature: mechanisms of diabetic cardiorenal complications and SGLT2i responses

Wenting Wang[1†], Yanfei Liu[2,3†], Qian Xu[1], Longkun Liu[1], Mengmeng Zhu[1], Yiwen Li[1], Jing Cui[1], Keji Chen[1] and Yue Liu[1,2,3*]

Abstract

Background Diabetic panvascular disease (DPD) is the leading clinical complication of diabetes mellitus (DM), characterized by atherosclerosis across multiple organ vessels. It is a major cause of high disability and mortality rates in DM. However, the pathological mechanisms and key mediators of DPD remain unclear.

Methods This study constructed a single-cell organotypic atlas of the vasculature containing 321,358 cells by integrating 14 single-cell datasets from 8 major mouse organs and tissues. A total of 63 cell types were identified, including 9 vascular cell subtypes, whereas the cell-to-cell interaction (CCI) patterns of the organotypic vasculature were systematically analyzed.

Results Endothelial cells (ECs) were identified as the major cell type involved in CCI within the vasculature, with their ligands interacting with receptors of various cell types, which contribute to multiple biological processes such as stem cell differentiation and immune regulation. Notably, the study examined the cellular communication characteristics of different EC subtypes. Additionally, the inter-organ communication between the heart and kidney—key tissues in DPD—was analyzed. The BMP signaling pathway emerged as a critical communication pathway leading to cardiorenal complications in DM, with SGLT2i having a regulatory role in BMP6 modulation.

Conclusions The study provides, for the first time, a single-cell analysis of the CCI patterns of the organotypic vasculature and highlights the central role of ECs. Moreover, the key role of BMP6 in diabetic cardiorenal complications is elucidated. These findings offer new insights into the mechanisms underlying DPD co-morbidities and provide a novel scientific basis for clinical prevention, treatment strategies for DPD, and the understanding of the action mechanism of SGLT2i.

Keywords Diabetic cardiorenal complications, Organotypic vasculature, BMP6, SGLT2i, CellChat

†Wenting Wang and Yanfei Liu contributed equally to this work

*Correspondence:
Yue Liu
liuyueheart@hotmail.com
[1]National Clinical Research Center for Chinese Medicine Cardiology, Xiyuan Hospital, Chinese Academy of Chinese Medical Sciences, Beijing 100091, China
[2]The Second Department of Geriatrics, Xiyuan Hospital of China Academy of Chinese Medical Sciences, Beijing 100091, China
[3]Key Laboratory of Disease and Syndrome Integration Prevention and Treatment of Vascular Aging, Xiyuan Hospital of China Academy of Chinese Medical Sciences, Beijing, China

© The Author(s) 2025. **Open Access** This article is licensed under a Creative Commons Attribution-NonCommercial-NoDerivatives 4.0 International License, which permits any non-commercial use, sharing, distribution and reproduction in any medium or format, as long as you give appropriate credit to the original author(s) and the source, provide a link to the Creative Commons licence, and indicate if you modified the licensed material. You do not have permission under this licence to share adapted material derived from this article or parts of it. The images or other third party material in this article are included in the article's Creative Commons licence, unless indicated otherwise in a credit line to the material. If material is not included in the article's Creative Commons licence and your intended use is not permitted by statutory regulation or exceeds the permitted use, you will need to obtain permission directly from the copyright holder. To view a copy of this licence, visit http://creativecommons.org/licenses/by-nc-nd/4.0/.

Introduction

Diabetes mellitus (DM) is a global chronic metabolic disease that imposes significant healthcare burdens, social costs, and premature mortality, which pose a critical threat to public health [1]. Among its most severe complications is diabetic panvascular disease (DPD), characterized by widespread atherosclerosis affecting both macrovessels and microvessels in the heart, brain, kidneys, eyes, and peripheral systems. Particularly, DPD impairs the function of many vital organs, such as the heart and kidneys [2]. The vasculature, one of the first functional systems to develop during embryogenesis, is also the first to be affected by DPD [3]. It primarily comprises two cell types: endothelial cells (ECs) lining the lumen and mural cells (pericytes and vascular smooth muscle cells [VSMCs]) surrounding the ECs [4].

As the innermost layer of the vasculature, ECs act as an important interface between organ parenchyma and circulating blood and regulate vascular tone, host defense, and metabolite exchange by sensing the circulatory environment [5, 6]. The heterogeneity and functional characterization of ECs are crucial for understanding physiological adaptation to the onset of diseases. Mural cells, which partially cover ECs, are essential for vascular formation and maturation. These cells influence EC behavior through cell-to-cell interactions (CCIs), thus regulating vascular stability, permeability, and remodeling [7]. Recently, significant evidence has highlighted the heterogeneity of vascular cells, particularly ECs, in aspects including morphology, gene expression, function, metabolism, and proliferative potential [8]. The recent development of single-cell RNA sequencing (scRNA-seq) has revolutionized the identification of vascular cell subtypes and the characterization of cellular heterogeneity in complex tissues with unprecedented resolution [9, 10]. However, current studies on EC have primarily focused on molecular characteristics and gene expression profiles of different EC subtypes, often overlooking their complex communication network with the vasculature's outer layer and the tissue microenvironment. This gap hinders a comprehensive understanding of vasculature physiological functions and the co-morbidity mechanisms underlying panvascular disease (PVD).

Multicellular organisms depend on cellular activity coordination, which is mediated by cellular communication networks among different cell types [11]. As a key interface between the circulatory system and various organ environments, the signaling interactions (e.g., CCI) of the vasculature have not been systematically explored to date. Identification of common CCI patterns and the underlying molecular mechanisms of the vasculature in both normal and diseased conditions could pave the way for developing more targeted and effective therapeutic strategies for PVD. This study systematically integrated and annotated single-cell transcriptomic data from eight tissues: the heart, brain, hypothalamus, lung, liver, kidney, aorta, and retina, sampled from young to old mice (4 weeks–96 weeks). This yielded 63 distinct cell types.

Based on cellular annotation, the cellular communication characteristics of the vasculature across tissues and cell types in different physiological states were comprehensively analyzed. High-frequency signaling pathways involved in EC communication shared across multiple tissues were identified. ECs were found to be the major cell type mediating CCIs in the vasculature, with their functions dependent on high-frequency receptor–ligand pairs. Moreover, varying degrees of CCI heterogeneity were observed across different EC subtypes.

Notably, we focused on the heterogeneity/conservativeness of communication in major target organs (heart and kidney) during DPD. Four significant communication modules were identified, and the roles of CCI mediators and sodium–glucose cotransporter 2 inhibitors (SGLT2i) in diabetic cardiorenal complications were verified. These findings provide valuable insights into the pathological mechanisms of DPD and offer guidance for the clinical treatment of diabetic cardiorenal complications.

Methods

Dataset resource

By manually searching the Gene Expression Omnibus (GEO) database using the keywords "scRNA-seq," "snRNA-seq," "single-cell RNA sequencing," and "single-nucleus RNA sequencing," a total of 14 mice scRNA-seq and snRNA-seq datasets were retrieved (Table S1). These datasets include 8 tissues from the heart, brain, hypothalamus, kidney, lung, liver, retina, and aorta, which covered an age span of 4 weeks–96 weeks.

scRNA-seq/snRNA-seq data preprocessing

Cell Ranger version 3.1.0 software (https://support.10xgenomics.com/single-cell-gene-expression/software/downloads/latest) was used to demultiplex the FASTQ reads and align them to the mouse transcriptome (mm10, provided by 10x Genomics) with the default parameters. The output of this pipeline contains a digital gene-barcode matrix for each sample. Then, all of the matrices were subjected to Seurat version 4.3 [12] for further data processing. Cells with more than 6,000 or less than 200 detected genes as well as those with a mitochondrial transcription ratio > 5% were discarded. Cell doublets (occasional pairs of cells that are not dissociated during sample preparation) were identified using the scDblFinder [13] and then discarded. After log(x + 1)-transformation, size factors were estimated using Scran version 1.16.0 [14], and normalization was performed.

Clustering based on the regulon matrix

We performed clustering on the normalized cell-gene matrix. Briefly, upon obtaining the matrix, the dimensionality was reduced by principal component analysis (PCA) based on the z-transformed expression levels of the identified regulons. Then, batch effects derived from technical and biological covariates, including the batch and harvested time, were corrected using harmony [15]. Next, the graph-based clustering of the PCA reduced data with the Louvain algorithm after computing the nearest neighbor graph was used to partition the cells. The resulting clusters were visualized in a 2-D embedding produced by uniform manifold approximation and projection (UMAP, version 0.4.6). Finally, the resulting coordinates of UMAP and cluster tags for each cell were assigned to the expression matrix after the size factor correction step for downstream analysis.

Estimation of the cell proportion

The significance of changes in the proportion of each cell type was calculated as described previously [16]. In brief, the detected number of each cell type was modeled as a random count variable using a Poisson process. The rate of detection was modeled by providing the total number of captured cells in a given mouse as an offset variable, with the condition of each mouse (wild-type or mutant) provided as a covariate.

Compositional analysis

We utilized the scCODA [17] software to assess changes in cell type proportions across different conditions. This tool employs a Bayesian framework to tackle the common challenge of low replication in single-cell studies. Specifically, it models cell-type counts with a hierarchical Dirichlet-Multinomial model. This model effectively accounts for the uncertainty in cell-type proportions and mitigates the negative correlative bias by simultaneously modeling all measured cell-type proportions. To guarantee a uniquely identifiable solution and enhance interpretability, scCODA selects a specific cell type as the reference (in our analysis, the 'reference_cell_type' parameter was set to 'automatic').

Cell-cell communication analysis

To elucidate the global communication patterns among cells, we employed CellChat [18] version 0.5.0, a computational tool designed to quantitatively infer cell-cell communication networks from single-cell RNA sequencing (scRNA-seq) data. This analysis was conducted using a curated list of ligand-receptor pairs provided by CellChat.

Overrepresentation test for gene ontology (GO) terms

We utilized g: Profiler [19] to conduct an overrepresentation analysis for differentially expressed genes (DEGs) identified in each cell type. The background gene set for the analysis consisted of all genes that were tested for differential expression within the respective cluster. Pathways exhibiting an adjusted *P*-value (false discovery rate, FDR) below 0.05 were considered significantly enriched.

GSEA enrichment

To investigate the broad signatures of cell-type-specific responses, we performed gene set enrichment analysis(GSEA) using the Python implementation of gseapy [20] version 0.10.1. The reference gene set collections H (hallmark gene sets) and C5 (ontology gene sets) were obtained from the Molecular Signature Database (MSigDB version 7.1) [21].

Protein-protein interaction (PPI) network construction

The STRING database was used to construction PPI network. Specifically, genes were upload and the 'Multiple protein' function was used. Next, the MCL clustering algorithm was used to cluster the network.

Animal experiments

Six-week-old male ApoE$^{-/-}$ mice (C57BL/6J) and male C57BL/6J mice were purchased from Jiangsu GemPharmatech Co. Ltd. (SCXK(SU)2018-0008). The mice were housed in a specific pathogen-free (SPF)-grade animal facility, provided with sterilized water and feed, at a temperature of 24 °C with a 12/12 h light cycle. After a 1-week acclimatization period, ApoE$^{-/-}$ mice were fed a high-fat diet (HFD), whereas C57BL/6J mice were fed a standard diet. After 6 weeks on the HFD, ApoE$^{-/-}$ mice received intraperitoneal injections of streptozotocin (STZ) (30 mg/kg/d) for 5 consecutive days to induce a type 2 diabetes mellitus (T2DM) model. C57BL/6J mice were injected with an equal volume of citrate solution as a control group (CON group).

The criteria for establishing the T2DM mouse model included a fasting blood glucose (FBG) level > 16.7 mmol/L, along with symptoms such as polyuria, polydipsia, and polyphagia [22]. The ApoE$^{-/-}$ mice were then randomly divided into two groups: the T2DM model group (T2DM group) and the dapagliflozin group (DAPA group). Mice in the DAPA group received dapagliflozin (DAPA) at 1 mg/kg/d via gastric gavage [23], while mice in the model and control groups received an equal volume of water via gastric gavage.

After eight weeks, the mice were sacrificed by intraperitoneal injection of sodium pentobarbital (30 mg/kg) following a 12-h fasting period. Blood, heart, and kidney tissues were then collected for further analysis. The animal experiment was approved by the Animal Ethics

Committee of Xiyuan Hospital, China Academy of Chinese Medical Sciences (Approval No. 2021XLC046-1).

Hematoxylin–eosin (H&E) staining

The whole hearts and kidneys of mice were fixed in 4% paraformaldehyde for 24 h at 25 °C. After fixation, the tissues were embedded in paraffin and sectioned at a thickness of 4 μm along the long axis. Paraffin-embedded tissue sections were deparaffinized using xylene and rehydrated through a graded series of alcohol concentrations. H&E staining was performed to assess structural changes in the heart and kidney tissues.

Tissue dissociation and cell isolation

Flash frozen heart tissue was homogenized in a Dounce homogenizer in Lysis Buffer with 1mM DTT and 1U/μL RNase inhibitor and incubated on ice for 5 min. The suspension was filtered through a 40 μm filter to remove debris and centrifuged at 4 °C 500 g for 5 min. After the nucleis were resuspended in 300 μL Lysis buffer and 300 μL RB buffer in a 2 mL tube, the mixture is centrifuged by density gradient to separate the nuclei from cell debris, collect the intermediate layer washed by RB buffer. Finally, the cell number and viability were assessed by an automatic cell counter.

Droplet-based snRNA-seq using the 10x genomics chromium platform

Single cells were suspended in PBS containing 0.04% BSA. snRNA-seq libraries were prepared using Chromium Single Cell 3′ Reagent Kits v2 (10x Genomics) according the manufacturer's protocol. The target cell recovery for each library was 6,000. The generated libraries were sequenced on an Illumina HiSeq2500.

Statistical analysis

Statistical analysis and data visualization were performed using GraphPad Prism (V9.5.0). Data are expressed as mean ± standard deviation (SD). For data that conformed to a normal distribution, comparisons between the two groups were conducted using a two-tailed Student's t-test. For data that did not conform to a normal distribution, the Mann-Whitney U test was used for comparisons between two groups. For comparisons across multiple groups, one-way analysis of variance (ANOVA) was used, followed by Bonferroni correction for multiple comparisons, provided the data met normality assumptions, otherwise, a Kruskal-Wallis test was applied. Statistical significance was defined as a $P < 0.05$. All independent experiments were repeated at least three times.

Results

Organotypic mapping of the vasculature using a single-cell approach

To comprehensively analyze the cellular composition and function of the organotypic vasculature, 14 published scRNA-seq and snRNA-seq datasets were integrated, which included 7 organs closely associated with vascular diseases—the heart, brain, lung, kidney, liver, hypothalamus, and retina—along with the aorta (Table S1A and B). After rigorous quality control and data integration, a single-cell organotypic atlas of the vasculature was constructed, comprising 321,358 cells from 56 mice across 43 samples (Fig. 1A). Clustering analysis, performed using UMAP, revealed 63 cell types, which were classified into tissue-specific and tissue-sharing cell types based on their distribution across tissues (Fig. 1B, Figure S1).

Regarding tissue-specific cell types, the kidney, hypothalamus, and retina, due to their unique anatomical structures, contributed to more distinct cell types, including podocytes, oligodendrocyte progenitor cells, and bipolar cells. For tissue-sharing cell types, six major categories were identified: ECs, immune cells, neurons, muscle/fiber cells, epidermal cells, and mural cells. Notably, ECs were further subdivided into lymphatic endothelial cells (EC lym., characterized by lgfbp5) and vascular EC (VEC, characterized by Alb), which were further classified into arterial EC (EC art.), vein ECs (EC vein), capillary ECs (EC cap.), and pericyte ECs (EC per., characterized by Emcn). Additionally, two specific EC subtypes were identified in the kidney: glomeruli ECs (EC glo.) and angiogenic ECs (EC ang.). To characterize the distribution of each cell type across organs, heat maps were generated to visualize the proportion of each cell type in different organs (Fig. 1C).

Shared cellular communication patterns in the organotypic vasculature

CCI is an essential process for maintaining life activities and responding to environmental changes in multicellular organisms [11]. To comprehensively characterize CCI in the organotypic vasculature, CellChat was used for the first time to map the CCI network across organs. Given the various shared cell types among multiple tissues, the cell types were initially classified based on the communication frequency pathways. The results showed that > 50% of the CCI pathways were found in only one to three organs (low-frequency CCI pathways), while only eight CCI pathways were shared across eight tissues (high-frequency CCI pathways). These high-frequency pathways included ANGPT, CDH, COLLAGEN, FGF, JAM, LAMININ, PECAM1, and PTPRM (Table S2A). This suggests that CCI is highly tissue-specific, with significant differences in communication patterns across tissues.

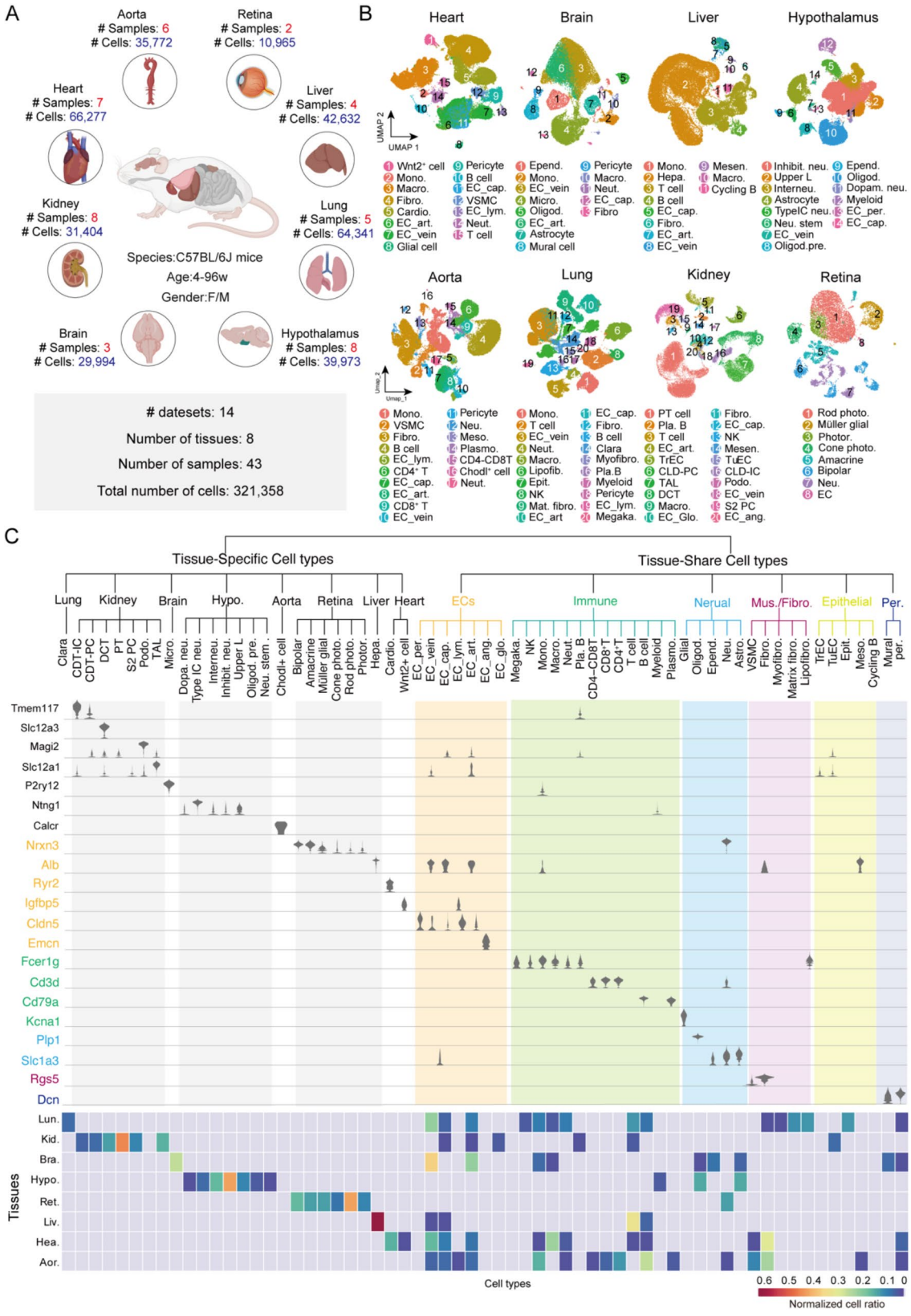

Fig. 1 (See legend on next page.)

(See figure on previous page.)

Fig. 1 Organotypic atlas of multiple vasculatures at a single-cell resolution. **A** Overview of scRNA-seq and snRNA-seq data of the 8 tissues included in the single-cell analysis, including cell count and number of samples. **B** Clustering plot using UMAP demonstrating the cell annotation results for each organ/tissue. Automated annotation with SingleR and manual annotation based on known biomarkers were performed. **C** Tree diagram visualizing the classification of all identified cell types, with major branches corresponding to the classification annotated in color. The expressions of the markers of each cell type across cells are indicated using violin plots, and a heat map was plotted down below to demonstrate the distribution ratio of each cell type among different organs. EC, endothelial cell; EC_art., arterial endothelial cell; EC_vein, vein endothelial cell; EC_lym., lymphatic endothelial cell; EC_cap., capillary endothelial cell; EC_per., pericyte endothelial cell; EC_ang. Angiogenic endothelial cell; EC_glo., Glomeruli endothelial cell; Mono., Monocyte; Macro., Macrophage; Megaka., Megakaryocyte; NK, Natural killer cell; Neut., Neutrophil; Pla. B, Plasma B cell; Plasmo., plasmoyte; Oligod.,Oligodendrocyte; Epend., Ependymal cell; Neu., Neuron; Astro., Astrocyte; VSMC, Vascular smooth cell; Fibro., Fibrolast; Lipofibro., Lipofibroblast; Matrix fibro., Matrix fibroblast; Myofibro., Myofibroblast; Meso., Mesothelial cell; Cycling B., Cycling basal cell; Epi., Epithelial cell; TuEC, Tubular epithelial cell; TrEC, Transitional epithelial cell; Per., Pericyte; CDT-PC, Collecting duct principal cell; CDT-IC, Collecting duct intercalated cell; DCT, Distal convoluted tubular cell; PT, Proximal tubule cell; Podo., Podocyte; S2PC, S2 proximal cell; TAL, Thick Ascending Limb cell; micro., microglial cell; Dopam. Neu., Dopaminergic neuron; Type IC neu., Type IC spiral ganglion neuron; Inhibit. Neu., Inhibitory neuron; Upper L., Upper layer cell; Interneu., Interneuron; Neu. Stem, Neural stem cell; Oligod. Pre., Oligodendrocyte precursor cell; Photo., Photoreceptor cell; Rod photo., Rod photoreceptor cell; Cone photo., Cone photoreceptor cell; Hepa., Hepatocyte; Cardio., Cardiomyocyte

To further analyze the functional differences between low- and high-frequency CCI pathways, GO enrichment analysis was performed for the genes encoding ligands of these pathways. The results showed that the ligands of low-frequency CCI pathways were strongly enriched in biological processes of inflammation, immunity, and cytokines, whereas the ligands of high-frequency CCI pathways were enriched in fundamental biological processes such as growth, development, differentiation, and organ formation (Fig. 2A, Table S2B). This finding suggests that low-frequency CCI pathways may be associated with tissue-specific immune regulation, whereas high-frequency CCI pathways may significantly contribute to maintaining basic biological functions. This study determined the cell types initiating CCI pathways with different frequencies in each tissue. The results indicated that most cell types initiated CCI pathways with a frequency > 3, albeit most of the CCI pathways were low-frequency.

Given the strong association of the ligands of low-frequency CCI pathways with inflammation and immunity, the study prioritized the proportion of immune cells in each tissue. The results showed that immune cells were > 35% of the population in three out of eight tissues, which was consistent with the frequency of immune-related CCI pathways (Fig. 2B). The immune system is the body's primary defense mechanism, tasked with recognizing foreign invaders and coordinating an immune response swiftly. Therefore, signaling mediators with high specificity are essential for the CCI pathways of immune cells, including soluble cytokines, chemokines, exosomes, and microvesicles [24, 25]. This partly explains the correlation between the number of low-frequency CCI pathways and the tissues with high immune cell ratios.

To better understand the distribution characteristics of CCI pathways with different sharing frequencies across tissues, the expressions of receptor and ligand genes associated with these CCI pathways in different tissues were further analyzed (Fig. 2C, Figure S2A, Table S2B). Notably, we found that as the sharing frequency increased, the expressions of cardiac and renal receptor genes also increased.

Moreover, the expression of high-frequency CCI receptors (e.g., Sdc1, Jam3, Dag1, etc.) was significantly higher than that of low-frequency CCI receptors (e.g., Adipor1, Cd40, Npr1, etc.) in multiple tissues, while no significant difference was observed in ligand expression (Fig. 2C, Figure S2A). This suggests that tissues require more pathways associated with basic life functions. Subsequently, receptor protein expression for different sharing frequencies in each was assessed using the tissue-based map of the human proteome [26] (Fig. 2D, Figure S2B). The results showed that receptor and ligand protein levels for high-frequency CCI pathways were higher than those for low-frequency CCI pathways in several tissues, which was consistent with the gene expression trend. The elevated expression of high-frequency receptor–ligand proteins significantly contribute to inter-tissue communication.

In addition, the vast differences in biological functions and tissue structures contribute to significant differences in CCI pathways across tissues (Figure S2C, D). For example, in the kidney, which contains specialized cells such as those in renal tubules and glomeruli, CCI primarily occurs via direct cellular contact, involving few CCI pathways [27]. Conversely, the aorta, the largest artery in the vasculature, has numerous cell populations and requires high-intensity CCI to regulate vascular tone and diastolic function [28, 29], thus involving several CCI pathways.

Characterization of receptor and ligand communication in multiple cell types of the organotypic vasculature

We have recognized identified eight inter-organ shared CCI pathways within the organotypic vasculature, which are largely mediated by receptors and ligands expressed in cell types common to all eight tissues. To explore these shared communication patterns, we examined the characteristics of the receptors and ligands in shared cell types across tissues (Fig. 3A). The results showed

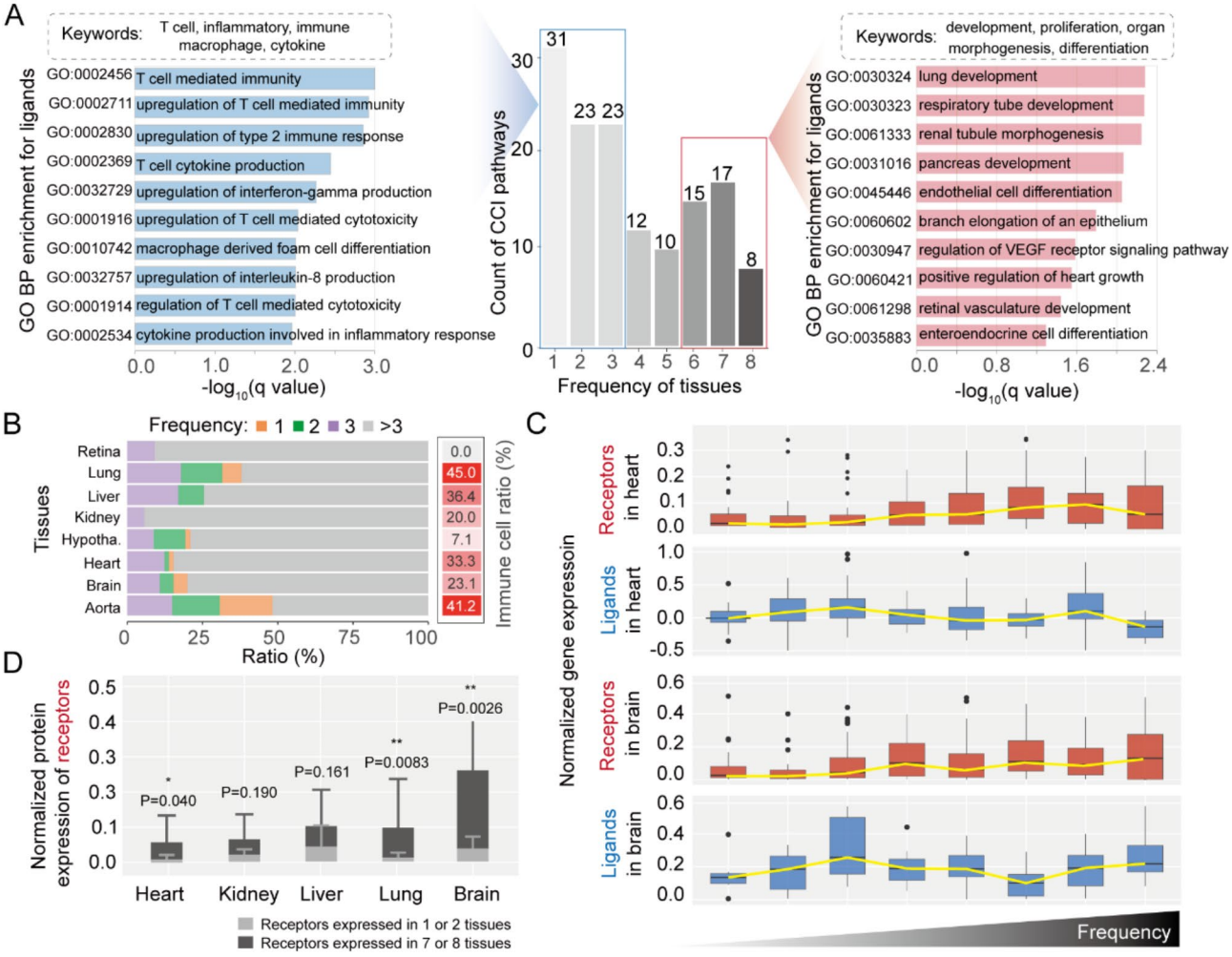

Fig. 2 CCI in the organotypic vasculature. **A** Classification (middle) and enrichment analysis (left and right panel) of ligands based on the frequency of inter-organ sharing of the CCI pathways, where blue boxes and bar graphs indicated the number of ligands and enriched entries of low-frequency CCI pathways (sharing frequency 1–3), and the red boxes and bar graphs indicated the number of ligands and enriched entries of high-frequency CCI pathways (sharing frequency 6–8); **B** Distribution ratio of cell types from ligands with different sharing frequencies among tissues and the right side showed the distribution ratio of immune cells in different tissues; **C** Expression of receptor and ligand genes of different sharing frequencies in the heart and brain. Bars from left to right indicated frequencies from 1 to 8. **D** Box plots indicating the expression of receptor proteins expressed in 1 or 2 tissues and that of receptor proteins expressed in 7 or 8 tissues, respectively, in each of the five tissues. Moreover, Student's t-tests were performed to assess the difference in protein expressions between the two groups, and the difference was determined using the *P*-value

that several shared ligand pairs and their functions were observed in all cell types. However, there are differences in the number of enriched terms for ligand genes among different cell types (Fig. 3B), which may contribute to the specificity of the CCI pathways (Figure S3A, B, and Figure S4A). For example, the specific CCI pathways in immune cells include pathways such as IL-6, CD226, and CCL, which are related to inflammation factors and immune responses [30, 31], while the CCI pathways in neuronal cells primarily involve MAG and ENHO pathways, which are associated with axon growth and neuronal function (Figure S3B) [32, 33].

Considering that the sharing between EC and immune-associated cells across tissues was the most frequent (Fig. 3C), we further explored the functions of the receptors and ligands in these two cell types. It was found that EC ligands may interact with receptors on multiple cell types, including stem, immune, and muscle cells, which were involved in multiple biological processes such as stem cell differentiation and immune regulation. In contrast, ligands from immune-associated cells primarily interact with other immune cells to ensure the precise regulation of the immune response (Fig. 3D). These CCI characteristics reflect the functional differences of distinct cell types in maintaining homeostasis.

To further explore the distribution characteristics of receptors and ligands across different tissues, we examined the cumulative distribution of receptors and ligands

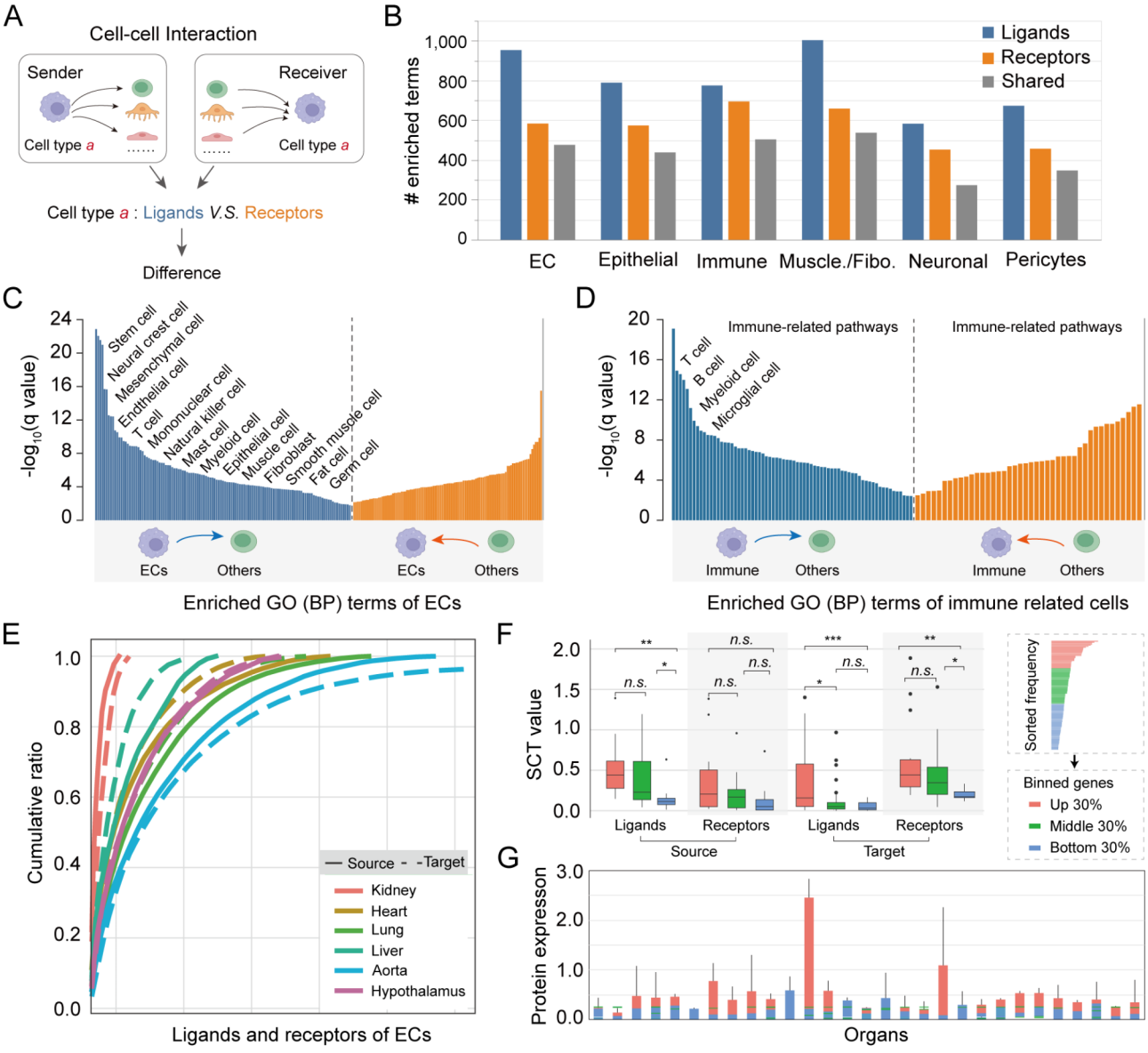

Fig. 3 Differences in receptor and ligand communication between different cell types in various tissues. **A** Schematic illustration of the study on the differences in receptor-ligand communication in different cell types. **B** The number of enriched pathways for specific receptors, ligands, and shared receptors and ligands in different cell subtypes. **C** Enriched GO BP entries involved in receptors and ligands emitting signals during CCI between ECs and other cell types. **D** Enriched GO BP entries involved in receptors and ligands emitting signals during CCI between immune-related cells and other cell types. **E** Cumulative percentage of frequency of occurrence of receptor/ligand in each organ with the total number of receptors and ligands of ECs. **F** All receptors and ligands were categorized into 3 categories based on the frequency of occurrence (right). Box plots indicated the expression of each category of receptor/ligand in single-cell sequencing data (Student's t-tests). **G** Protein expression of the 3 categories of receptor/ligand genes in each organ

in ECs, immune-related cells, fibroblasts, and neurons in each tissue (Fig. 3E, Figure S4B-D). The results revealed that the vascular tissue contained the highest number of receptors and ligands from structural cells, including ECs and fibroblasts [34, 35] (Fig. 3E, Figure S4C). This finding aligns with previous studies, indicating that ECs and fibroblasts significantly contribute to maintaining vascular structure and function.

Additionally, the aorta and lungs were rich in the receptors and ligands of immune cells (Figure S4B). The aorta, as a vascular tissue, is continuously exposed to shear and metabolic stresses, thus regulating the migration and activating immune cells, such as monocytes, in the blood vessels to maintain vascular homeostasis [36, 37]. Similarly, the lungs are enriched in immune cells, including macrophages, dendritic cells, and T cells, owing to their direct exposure to the external environment, where they perform immune defense functions [38]. Notably, among all tissues, neurons were only identified in the brain, hypothalamus, retina, and aorta. However, the

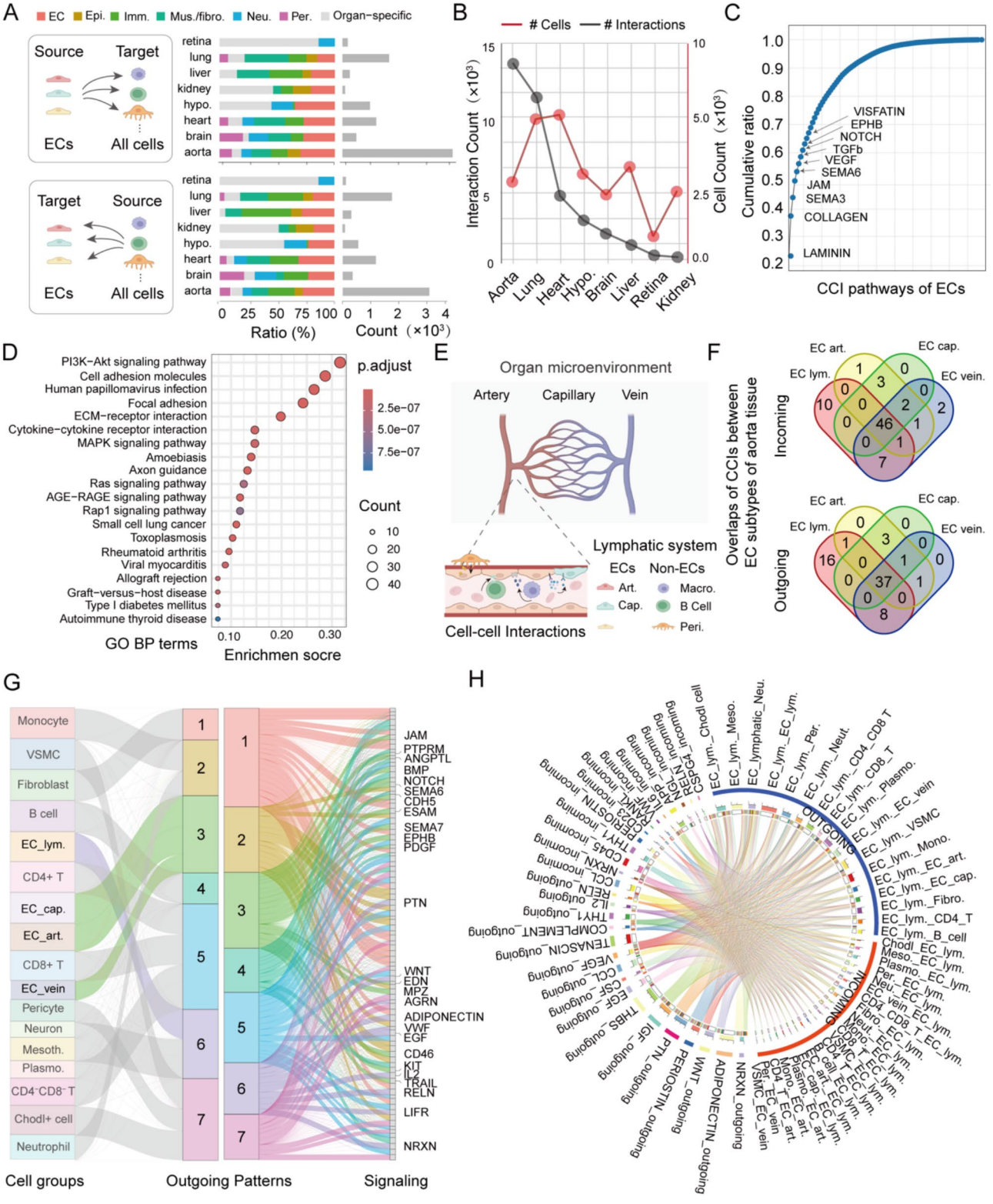

Fig. 4 (See legend on next page.)

(See figure on previous page.)

Fig. 4 Characterization of CCI of EC subtypes across tissues. **A** Proportion and number of CCIs of ECs as source and target with other cell types in 8 tissues. **B** Comparison of the number of cells and the number of CCIs in each tissue. **C** Cumulative frequency of CCI pathways of ECs. Names of top 10 pathways were labeled. **D** Enriched GO BP terms of receptor-ligand pairs in the CCI of ECs. **E** Classification of EC subtypes. **F** Venn diagram demonstrating the sharing of CCI pathways of the incoming and outgoing signaling of different EC subtypes in the aorta. **G** Sankey diagram demonstrating the cellular communication patterns and pathways of different cell types in the aortic tissues, and the key pathways in the communication modules involving EC subtypes were labeled. **H** The outermost circle in the circle diagram indicated the names and directions of CCI pathways in the aorta. The middle circle indicates the CCI information and the signaling direction of the CCI pathway of the specific pathway involved, and the inner circle indicates the strength of CCI after treatment with $-\log_{10}$ (communication probability) for each cellular communication. The connecting lines indicate CCI and the color shade indicates CCI strength. EC, endothelial cell; EC_art., arterial endothelial cell; EC_vein, vein endothelial cell; EC_lym., lymphatic endothelial cell; EC_cap., capillary endothelial cell; Mono., Monocyte; Per., Pericyte; VSMC, Vascular smooth cell; Fibro., Fibrolast

aorta exhibited an almost complete absence of receptors or ligands for neurons (Figure S4D). This finding suggests that although each cell type has unique communication pathways, the overall organ function may primarily depend on receptor–ligand pairs with high-frequency expressions.

To test this hypothesis, we examined the expression levels of receptor–ligand pairs with different frequencies, using the heart as an example. The results showed that the expression levels of high-frequency receptor–ligand pairs were significantly higher than those of low-frequency pairs, regardless of whether the cells acted as signal senders or receivers (Fig. 3F). This finding suggests that high-frequency receptor–ligand pairs may be the primary drivers of the heart's basic functions. Further observations of the expressions of receptor–ligand protein expression in each tissue produced similar results (Fig. 3G). These findings suggest that in healthy conditions, organ function primarily depends on high-frequency receptor–ligand pairs, whereas low-frequency receptor–ligand pairs may contribute to specific pathological conditions or unique physiological events. Notably, under disease conditions, high-frequency receptor–ligand pairs could be the key targets for addressing multi-organ co-morbidities.

Characteristics of CCI of ECs in the organotypic vasculature

ECs are the only cell type common to all tissues, and the analysis of communication patterns and receptor–ligand characteristics highlights their fundamental, extensive, and central role in the CCI of the organotypic vasculature. To further analyze the communication characteristics of ECs, the CCI strength of ECs as signal sources (senders) and targets (receivers) were statistically analyzed across eight tissues (Fig. 4A, Figure S5A, B), in order to gain a comprehensive understanding of the communication characteristics of ECs in the organotypic vasculature at the tissue level, including their specific roles and primary communication targets. The results showed that the number and proportion of incoming and outgoing signals for ECs were similar in each organ, with outgoing signals constituting the majority. The main targets of EC communication were vascular structural cells, including fibroblasts, pericytes, and ECs themselves.

Notably, the number of EC communications differed significantly between tissues. To exclude the effect of cell numbers on communication distribution, the correlation between cell numbers and communication frequency in each tissue was analyzed (Fig. 4B). The results indicated that CCI distribution was independent of cell count but closely related to the specific physiological functions and microenvironments of each tissue. For example, despite similar cell counts in the aorta and kidney, EC communications were observed to be more frequent in the aorta, this observation is consistent with the aorta's physiological role as a major artery, which requires intense CCI to maintain vascular tone and diastolic function [39–41].

To further explore the communication pathways of ECs, the primary communication pathways of ECs in the organotypic vasculature were analyzed (Fig. 4C). The analysis revealed that LAMININ, COLLAGEN, and JAM associated with the basement membrane and cell adhesion—were the major pathways of EC communication. Moreover, functional enrichment analysis of receptors and ligands revealed that EC communication was closely related to the PI3K-Akt signaling pathway, cell adhesion molecules, and extracellular matrix (ECM)-receptor interactions (Fig. 4D). These findings indicate that ECs play a critical role in maintaining vascular and tissue homeostasis through processes such as tissue repair, cell migration, and immune response.

EC are among the most abundant and heterogeneous cell types in the body. Based on function and structure, they can be categorized into VEC and EC lym. VECs are further categorized into EC art., EC-vein, and EC-cap [42]. Although existing studies have highlighted tissue specificity and gene expression profiles of each EC subtype, the cellular communication patterns among these subtypes remain unexplored. Therefore, the CCIs of various EC subtypes across tissues were analyzed (Fig. 4E). The results revealed both shared CCI pathways as well as unique CCI pathways in incoming and outgoing signaling of different EC subtypes across tissues (Fig. 4F, Figure S5C, D). For example, in the aorta, VECs (including EC art., EC vein, and EC cap.) were primarily involved in BMP, JAM, and NOTCH signaling pathways associated with angiogenesis. Conversely, EC-lym showed communication patterns resembling those of mesothelial cells

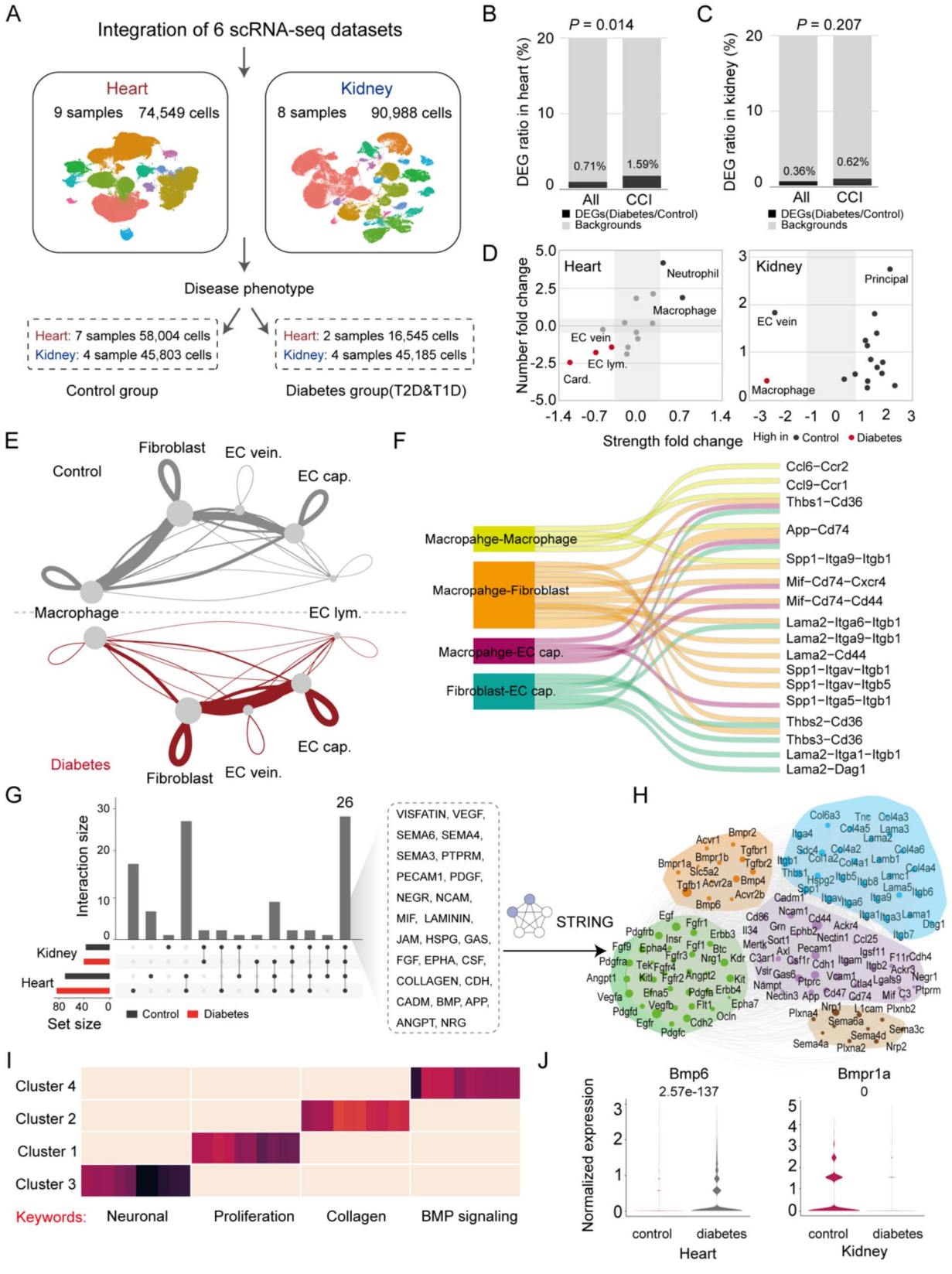

Fig. 5 (See legend on next page.)

(See figure on previous page.)

Fig. 5 Changes of CCI in the heart and kidney during DM. **A** Overview of the number of cells and samples of the heart and kidney for scRNA-seq included in the analysis. **B** Proportion of DEG genes (Diabetes/Control) in all pathways and CCI-related pathways in the heart. **C** Proportion of DEG genes (Diabetes/Control) in all pathways and CCI-related pathways in the kidney. **D** Scatter plots of FC intensity values and summed FC values of individual annotated cells in the heart and kidney. **E** Comparison of CCI strength in the heart, macrophages, and fibroblasts between control and DM groups. **F** Sankey diagram demonstrating the cell types and the specific receptor-ligand pairs with large changes in communication strength under disease conditions in Figure **E**. **G** UpsetR plot for screening the 26 intersecting CCI pathways between diabetes and control groups. **H** PPI plots of receptor and ligand genes in the intersecting CCI pathways based on the PPI intensity through the STRING database. The genes were categorized into 4 clusters based on the interaction intensities. **I** The individual CCI/enrichment pathways involved in the genes of the 4 clusters were screened, summarized, and demonstrated using heatmaps. **J** Violin plots of the expressions of Bmp6, the core gene of the module, and its receptor Bmpr1a in the heart and kidney in normal conditions and DM, as derived from integrated transcriptomic datasets. The intergroup differences in the expression were indicated by using the *P*-value of the Wilcox rank sum test

and neurons, primarily participating in lymphoid development and immunoregulatory signaling, such as RELN, IL2, and NRXN (Fig. 4G, F). These findings highlight the functional heterogeneity of ECs from a communication perspective and offer new insights into their tissue-specific functions within the organotypic vasculature.

Changes in the CCI of the heart and kidney during DM

The shared CCI patterns of the panvascular system and their mediators across tissues under physiological conditions have been explored. However, in complex, high-mortality diseases, simultaneous or sequential pathologic changes across multiple organs often involve intricate intercellular interference mechanisms that remain largely unknown. DPD is a vascular disease characterized by widespread atherosclerosis in patients with diabetes, affecting multiple critical target organs, including the heart, kidneys, and brain [2]. Highly complex interactions are observed in the heart and kidneys, the organs most affected by DM [43]. Over 40% of patients with diabetes experience heart failure, and nearly half of patients with heart failure suffer from chronic kidney disease [44].

Understanding the mechanisms behind cardiorenal complications is essential for revealing DPD pathogenesis. To analyze CCI changes in the heart and kidney during DM, four additional single-cell datasets from mice with diabetes were selected (Table S3), along with two heart datasets from the previously mentioned single-cell organotypic atlas of vasculatures and categorized into control and diabetes groups. The CCI changes in the heart and kidney between control and diabetic conditions were visualized using CellChat to explore the key communication mediators of diabetic cardiorenal complications (Fig. 5A, Figure S6A).

The results showed that DM significantly changed the CCI patterns of the heart and kidney. Specifically, among all pathways enriched with differentially expressed genes (DEGs) (Diabetes group vs. Control group), diabetes-induced DEGs accounted for a higher proportion of CCI-related pathways, suggesting that intercellular interactions play an important role in the pathological processes of diabetes-induced heart disease. Conversely, the CCI of renal cells was less responsive to diabetes (Fig. 5B, C). Further analysis revealed that the CCI of macrophages, EC vein, and EC lym. in the heart was significantly affected by DM, which aligns with previous findings showing that DM alters the function and structure of the heart by changing the communication patterns of these key cells [45]. However, in the kidney, macrophages and EC veins were more affected by DM (Fig. 5D, Figure S6B, C), Additionally, we found that organ-specific cell types, such as cardiomyocytes in the heart and principal cells in the kidney, exhibited smaller changes in quantity and strength of CCI compared to ECs and immune cells. This suggests that organ-specific cell types may retain their core intercellular signaling structures to combat the pathological microenvironment changes in DM. In contrast, ECs and immune cells showed significant alterations in communication, who act as primary drivers of diabetic tissue injury through dynamic CCI remodeling.

Notably, although the magnitude of CCI changes in the fibroblasts of the heart and kidney was small, the number of such CCIs was significantly higher than in other cell types (Fig. 5D, Figure S6B, C). Fibrosis is one of the common pathological mechanisms in diabetic heart disease and diabetic nephropathy [46]. Substantial evidence indicates that diabetes-associated fibrogenesis is primarily driven by hyperglycemia-induced fibroblast activation, with ECs and macrophages identified as key cellular sources of pro-fibrotic mediators [45, 47, 48]. These cells orchestrate fibroblast phenotypic modulation through paracrine signaling and direct Intercellular interactions, thereby promoting fibrotic responses characterized by excessive extracellular matrix synthesis and collagen deposition [49, 50]. We speculate that the high CCI count of fibroblasts may be related to their response to communication signals emitted by ECs and immune cells.

To further understand the aberrant communication mechanisms in the heart and kidney during DM, the CCIs between macrophages, fibroblasts, and various EC subtypes were analyzed in detail (Fig. 5E, Figure S6D). In the heart, DM reduced the crosstalk between fibroblasts and macrophages, with receptor–ligand pairs associated with immune cell infiltration and fibroblast activation (e.g., Mif-CD74_Cxcr4 and Spp1-Itga9_Itga1)

significantly reduced. Conversely, the CCI between fibroblasts and EC cap. increased, accompanied by an increase in receptor–ligand pairs involved in angiogenesis and ECM remodeling (Fig. 5F).

In the kidney, DM primarily enhanced the crosstalk between different EC subtypes, leading to a significant increase in receptor–ligand pairs related to collagen fiber formation, including Col4a3-Cd44 and Col4a3-Itga1_Itgb1 (Figure S6D, E). These changes indicated that diabetes promotes renal fibrosis and vascular remodeling by altering the communication patterns between different EC subtypes.

To identify key communication pathways involved in diabetic cardiorenal complications, we selected 26 CCI pathways that exhibit changes in both the heart and kidney under diabetic conditions (Fig. 5G). Subsequently, we employed the STRING database to perform PPI and enrichment analyses of the corresponding receptor–ligand genes within these pathways (Fig. 5H, I). The results showed that these pathways primarily involved four key modules: BMP signaling, collagen synthesis, neuron-related signaling, and angiogenesis (Figure S6F). Key nodes in each module, such as Bmp6, Tgfb1, Col4a1, and Egfr, may contribute to the cardiorenal complications of DM.

Further analysis of the gene expression levels of these core receptor–ligand pairs in the heart and kidney, as obtained from the database, showed that Bmp6 and its receptor Bmpr1a were significantly altered in diabetic hearts and kidneys (Fig. 5J, Figure S6G). These genes could be potential targets for diabetic cardiorenal complications.

BMP signaling mediates aberrant CCI in diabetic cardiorenal complications and the significant effect of SGLT2i

Hyperglycemia-induced cardiorenal damage is well established. DM doubles the risk of cardiorenal syndrome and significantly increases the risk of adverse cardiovascular events, end-stage renal disease, and death [51]. Therefore, developing comprehensive therapeutic strategies for diabetic cardiorenal complications is crucial to improving patient outcomes and prognosis. Large clinical studies have demonstrated that the antihyperglycemic agent SGLT2i effectively reduces the risk of heart failure and improves renal outcomes, including end-stage renal disease, elevated creatinine, and death from nephropathy [52–54]. To further validate the role of the identified key communication signals in diabetic cardiorenal complications and to explore the mechanisms underlying the cardiorenal benefits of SGLT2i from a CCI perspective, we selected $ApoE^{-/-}$ mice with a background of lipid metabolism disorders (C57BL/6J genetic background) as model mice. T2DM was quickly induced by intraperitoneal injection of low-dose STZ and HFD feeding [55], and DAPA was used as a therapeutic intervention (Fig. 6A).

The results showed that mice in the T2DM group exhibited significant weight loss and had markedly elevated blood glucose levels compared to the CON group, along with pathological changes in cardiac and renal tissues, including myocardial fracture and deformation, increased glomerular volume, and infiltration of inflammatory cells. After treatment with DAPA, the blood glucose levels of mice in the DAPA group were restored to normal, whereas the pathological changes in cardiac and renal tissues were significantly improved, with clear morphology and arrangement of cardiomyocytes, as well as critical improvement in glomerular hypertrophy and inflammatory cell infiltration (Fig. 6B-D, Fig.S7, TableS4). Also, while we did not conduct additional measurements of the renal parameter differences between the mouse groups, previous studies have demonstrated that DAPA exhibits significant individual renal protective effects in T2DM mice, including reducing the urine albumin/creatinine ratio and serum urea levels [56].

To further analyze the effects of T2DM and SGLT2i treatment on the CCI between cardiac and renal cells, snRNA-seq of mouse hearts was performed, and intergroup differences in the strength and number of CCIs were compared using CellChat. We focused on the CCI pathways that were abnormal due to T2DM and were normalized by DAPA treatment. The results revealed that the LAMININ, PTPRM, and COLLAGEN pathways had high scores of CCI strength but few interactions. Conversely, numerous interactions were observed in the SEMA3, ADGRG, and ADGRL pathways, although their interaction strength was significantly reduced (Fig. 6E). Notably, both the strength and number of interactions of the BMP pathway were significantly higher than average, suggesting its critical role in CCI during diabetic cardiorenal complications.

Subsequently, differential expression levels of receptor–ligand genes in these pathways were analyzed, thus revealing the most significant changes for the ADGRG, SEMA3, and BMP pathways (Fig. 6E). Particularly, the receptor–ligand genes of the BMP signaling pathway were significantly upregulated in the T2DM group and downregulated in the DAPA group (Fig. 6F). These results align with earlier findings and further confirm the central role of BMP signaling in diabetic cardiorenal complications [57].

To further validate the role of BMP signaling in the cardiorenal protective mechanism of SGLT2i, changes in key pathway BMP molecules in the heart were analyzed. The results showed that BMP6 and its receptor Bmpr1a were significantly upregulated in the T2DM group and downregulated in the DAPA group (Fig. 6F). This was consistent with previous findings on diabetic nephropathy [57],

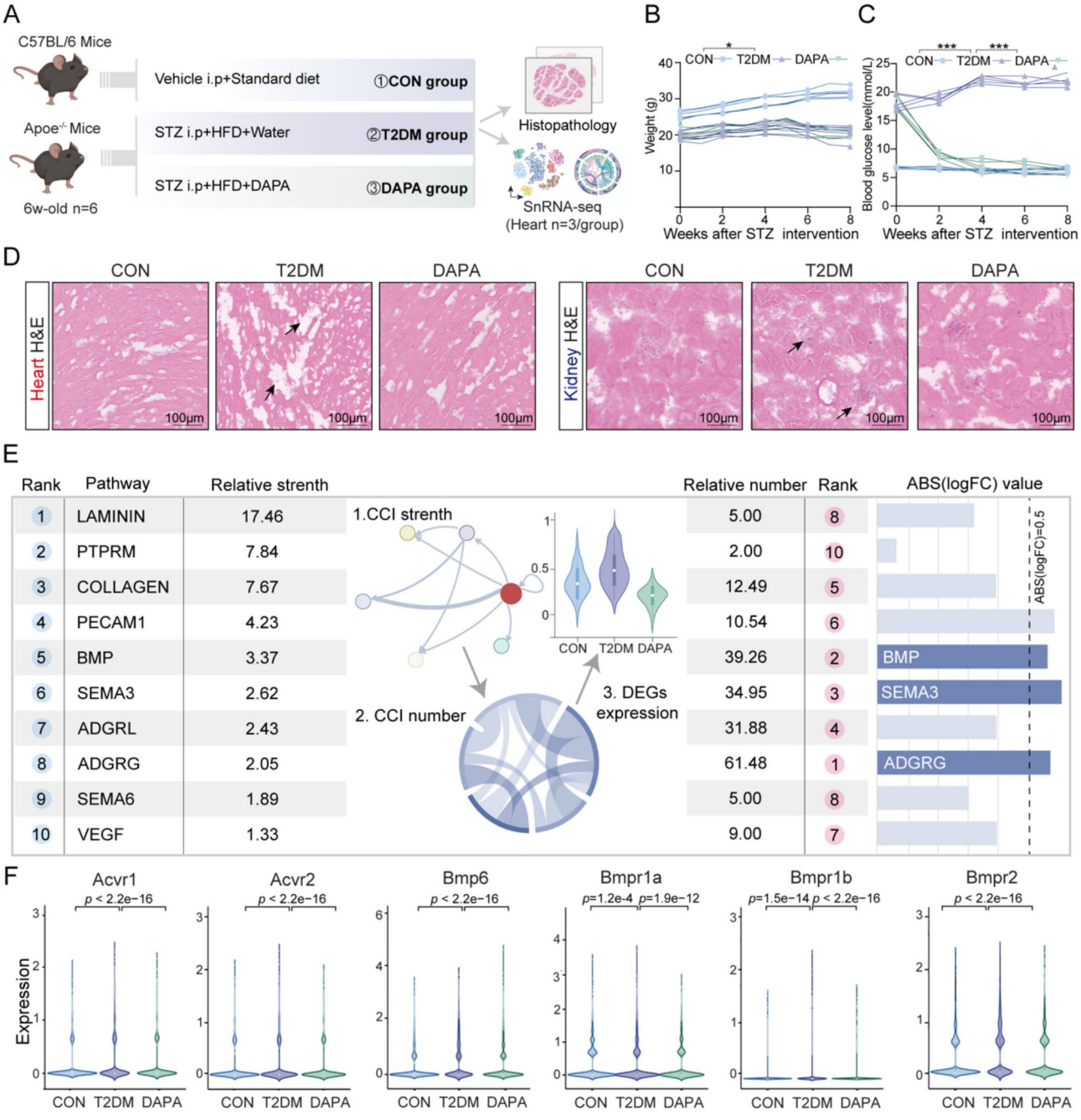

Fig. 6 Changes in CCI networks in DM and during treatment. **A** Schematic diagram of animal experiments. Specifically, STZ combined with 8 weeks of HFD feeding was used to construct a mouse model of T2DM. The intervention was performed with control or DAPA for 8 weeks before histopathology examinations for heart and kidney ($n=6$). SnRNA-seq assay was performed for the heart ($n=3$). **B** Changes in weight after diabetes establishment for each group of mice ($n=6$, one-way ANOVA, $^{***}P<0.001$). **C** Changes in FBG levels after diabetes establishment for each group of mice ($n=6$, one-way ANOVA, $^{***}P<0.001$). **D** Representative images of H&E pathological staining of heart and kidney tissues in each group of mice ($n=3$, 20×), arrows indicate the areas of myocardial fracture or the locations of enlarged glomerular units, all biological replicates are provided in Fig.S7. **E** Screening of key communication pathways during DM and DM treatment based on the strength of CCI, the number of CCIs, and the differential gene expression levels of receptor-ligand pairs in different groups. **F** Gene expression levels of receptor-ligand pairs in the BMP pathway in the heart of each group of mice ($n=3$, one-way ANOVA)

suggesting that BMP6 may be a novel target for the cardiorenal protective mechanism of SGLT2i. Our analysis indicates that SGLT2i may restore abnormal CCI in the heart and kidney in DM by regulating the BMP signaling, thus exerting protective effects on both organs. This provides new insights into the cardiac and renal benefits of SGLT2i and offers a potential target for developing precise therapeutic strategies against cardiorenal complications in DM.

Discussion

The vasculature plays a crucial role as a barrier and a distributed organ in maintaining the normal function of various organs and tissues in a healthy state. However, dysfunction of vascular-related cells, particularly in pathological conditions, significantly contributes to vascular pathologies including atherosclerosis, which can lead to PVD. Although endothelial dysfunction and hypoxia [58, 59] are known pathogenic mechanisms of PVD, current endothelial protective agents, and anti-hypoxic therapies have shown limited clinical efficacy. Therefore, a deeper understanding of the vasculature's functional characteristics and its changes in pathological states is essential for optimizing existing treatments and developing new therapeutic strategies.

This study systematically explored the CCI patterns of the organotypic vasculature from a single-cell perspective for the first time and demonstrated the central role of ECs in the intercellular signaling within the vasculature using a frequency-based mathematical model. These findings offer a crucial foundation for understanding the common physiological mechanisms of the panvascular system.

The dynamic network of CCI and inter-organ collaboration is essential for maintaining organ function and microenvironment homeostasis. Over the past decade, several computational tools, including CellphoneDB [60], ICELLNET [61], and CellChat [18], have been developed to infer CCIs from gene expression data and enable detailed characterization of CCI networks in key target organs [62–64]. However, most studies have focused on CCIs within specific organs under physiological or pathological conditions. This has left a gap in understanding inter-organ communication and collaboration. By integrating scRNA-seq/snRNA-seq data from multiple organs, we demonstrated the feasibility of quantifying multi-organ CCI for the first time. Our analysis identified numerous specific CCI pathways and a few overlapping CCI features across different organs to highlight key inter-organ communication mechanisms.

Based on the frequency-based mathematical model, pathways essential for life activities, such as cell development and differentiation, were found to overlap across all organs. This aligns with the well-established concept that despite differences in function and morphology, organs share a common evolutionary trajectory in basic signaling and biological processes [65]. Notably, immune-related CCI pathways were significantly increased only in organs with high immune requirements (e.g., lung, aorta, and liver). Previous studies have demonstrated that CCI in immune cell populations is primarily driven by specialized receptors and secreted ligands, which are numerous in immune system-related organs than in non-immune organs [66]. Our study supports these findings. Additionally, we identified various shared receptor–ligand pairs across different cell types, which may explain the inter-organ CCI signaling. Notably, high-frequency receptor–ligand pairs (e.g. Lama4-Dag1, Col4a1-Sdc1, etc.) were expressed at significantly higher levels than low-frequency pairs (e.g. Adipoq-Adipor1, Cd40lg-Cd40, etc.,) across various organs and cell types. This suggests that high-frequency receptor–ligand pairs play a dominant role in intercellular signaling within the vascular system. Therefore, these high-frequency receptor–ligand pairs may be potential targets for the development of PVD drugs.

As the innermost layer of the vasculature, ECs serve as the interface for communication between the vascular system and external environment, playing a critical role in maintaining vascular homeostasis. This includes regulating blood pressure and blood flow, influencing angiogenesis, changing vascular permeability, and mediating immune and inflammatory responses. Therefore, abnormalities of the ECs would directly impact the vascular system and lead to the development of vascular diseases. For example, endothelial dysfunction is the earliest detectable pathologic change in atherosclerosis [67]. In DM, hyperglycemia first causes abnormalities in EC metabolism and then vascular damage [68].

By analyzing the communication patterns and characteristics of receptors and ligands of the organotypic vasculature, the intra- and inter-organ communication characteristics of ECs were summarized for the first time. We found that ECs mainly acted as signal senders in the organotypic vasculature, whereas their ligands are more likely to interact with receptors of vascular structural cells, such as fibroblasts, pericytes, and ECs themselves. LAMININ, COLLAGEN, and JAM, which are associated with the cell basement membrane and cell adhesion, are the main communication pathways of EC. They include PI3K-Akt signaling, cell adhesion molecules, ECM-receptor interactions, and other biological functions. This finding is consistent with a recent study on the organotypic atlas of vascular cells. Specifically, various vascular and organotypic communication pathways related to cell adhesion signaling are observed across ECs and their surrounding cells in vascular beds and tissues [69].

Additionally, significant differences were observed in the communication patterns between different EC subtypes. For example, BMP and NOTCH signaling pathways, which are closely related to angiogenesis, were predominantly observed in VECs, while immune-related signals such as RELN and IL2 were primarily specific to EC lym. These findings highlight the functional heterogeneity of ECs from a communication perspective and offer new insights into understanding the tissue-specific functions of ECs in panvascular organs.

Another key outcome of this study was the exploration of common changes in the communication between the heart and kidney during DM. We present the first quantitative analysis of CCI in both the hearts and kidneys of diabetic mice, focusing on the shared intercellular communication changes in a diabetic context. The heart was more sensitive to the diabetic environment and exhibited more changes in CCI than the kidney. Previous studies revealed significant changes in the number and abundance of metabolites in the heart in response to DM, and our results further support this finding [70].

Specifically, this study revealed several CCIs across various EC subtypes in the heart and kidney during DM, along with a significant increase in receptor–ligand pairs associated with angiogenesis, basement membrane formation, and fibrosis. These findings suggest that EC dysfunction contributes to initiating vascular complications in DM [71, 72]. Further analysis of the communication pathways and the corresponding functions of receptors and ligands in both the heart and kidney during DM highlighted BMP signaling as a key factor in the cardiorenal complications of DM. BMP is a subgroup of the transforming growth factor β (TGFβ) superfamily, and its signaling pathways include both the classical Smad-dependent pathway and non-classical Smad-independent pathways, both of which are involved in bone formation as well as the development of organs such as the heart and kidney [73]. Numerous studies have demonstrated the significant role of BMP signaling in DM and vascular complications [74, 75].

Activation of BMP signaling triggers the endoplasmic reticulum stress response in pancreatic islets, which promotes dysfunction of pancreatic β-cell dysfunction and elevated glucose levels [76]. Elevated BMP levels are positively associated with the development of coronary artery disease in DM, vascular calcification, diabetic retinopathy, and diabetic nephropathy [77–79]. Our analysis also revealed that the expression of BMP6, a key molecule in BMP signaling, was significantly increased in the heart during DM, which further supported the key role of BMP signaling in the cardiorenal complications of DM.

CCI is a key mechanism for maintaining organismal adaptation and homeostasis in multicellular organisms. Changes in CCI have been identified as key contributors to organ co-morbidities, which offer new perspectives for drug development and application. The cardiorenal benefits of SGLT2i, a first-line hypoglycemic agent, are well-supported by clinical evidence, which demonstrates potential cardiorenal protection by improving metabolic communication in the kidney and regulating the gut-renal axis [70]. However, the effect of SGLT2i on the CCI between heart and kidney cells remains unclear. By combining our analysis of shared CCIs between the heart and kidney during DM, we explored the cardiorenal protective mechanism of SGLT2i from a CCI perspective. Using the heart as an example, we performed SnRNA-seq and CCI analyses by focusing on the CCI pathways restored by DAPA treatment.

Notably, the BMP signaling pathway emerged as a critical mediator of cardiorenal CCIs in DM, as indicated by its prominent ranking in terms of CCI strength, number, and magnitude of changes. Previous studies have demonstrated that SGLT2i improved aberrant CCIs in diabetic nephropathy and inhibited EC-derived Bmp6 signaling [35]. Based on the inhibitory effects of DAPA on the receptors and ligands of the BMP signaling pathway in the heart, we hypothesize that SGLT2i may restore the disrupted CCI between the heart and kidney in DM by regulating BMP signaling to achieve the potential protection of the heart and kidney.

Overall, we explored the CCI patterns in panvascular organs under normal conditions and during DM, which offer new insights into the physiological mechanisms of the panvascular system and the characteristics of DPD. We highlighted the key role of BMP signaling in diabetic cardiorenal complications and the protective effects of SGLT2i. Moreover, this study introduced a mathematical model and algorithm based on frequency screening to quantify cell-type interactions across organs and identify key CCI pathways and receptor–ligand pairs. This novel research paradigm can guide future investigations into CCI in multiorgan and panvascular lesions and inform the development of drugs targeting CCI mediators.

However, while we focused on communication abnormalities in diabetic cardiorenal complications and the systemic effects of DAPA, the lack of deeper exploration of specific injury-associated cell subtypes remains a limitation. Future studies integrating spatial omics could further dissect the cellular drivers of Diabetic cardiorenal complications and the cardiorenal benefits of SGLT2i.

Conclusion

This study constructed a comprehensive organotypic single-cell atlas of the vasculature by integrating scRNA-seq data from eight organs and systematically analyzed vascular CCI characteristics. A frequency-based mathematical model highlighted the critical role of high-frequency receptor–ligand pairs in organ function specificity and

multi-organ co-morbidities. Moreover, the core role of ECs in vasculature was identified. Using the heart and kidney as examples, BMP6 was shown to promote cardiorenal complications and mediate the protective effects of SGLT2i. These findings provide a scientific basis for understanding DPD comorbidity mechanisms and the action mechanism of SGLT2i.

Abbreviations

CCI	Cell-to-cell interaction
DM	Diabetes mellitus
DPD	Diabetic panvascular disease
EC	Endothelial cell
ECM	Extracellular matrix
FBG	Fasting blood-glucose
GEO	Gene Expression Omnibus
GO	Gene Ontology
HFD	High-fat diet
PPI	Protein-protein interaction
PVD	Panvascular disease
SGLT2i	Sodium–glucose cotransporter 2 inhibitors
T2DM	Type 2 diabetes mellitus
UMAP	Uniform Manifold Approximation and Projection
VSMC	Vascular smooth muscle cells

Supplementary Information

The online version contains supplementary material available at https://doi.org/10.1186/s12933-025-02655-2 .

Supplementary Material 1

Supplementary Material 2

Supplementary Material 3

Supplementary Material 4

Supplementary Material 5

Author contributions

YL responsible for conceptualising this paper. WTW, YFL, QX and LKL were responsible for data curation. WTW, YFL, QX, MMZ, YWL and JC accessed and verified the underlying data and did the analysis. WTW and YFL were responsible for data visualisation. WTW and YFL were responsible for writing the original draft. YL and KJC reviewed and edited the draft. YL was responsible for supervision and project administration. The authors had unrestricted access to the study data and retained ultimate responsibility for the decision to submit the paper for publication.

Funding

This work was supported by Excellent Young Science and Technology Talent Cultivation Special Project of CACMS (CI2023D006), National Outstanding Youth Natural Science Foundation of China (82022076), and Hospital capability enhancement project of Xiyuan Hospital of CACMS. (NO. XYZX0201-10).

Availability of data and materials

The snRNA-seq data for mouse heart tissue are deposited in the NGDC database under accession number PRJCA035854. The details of the datasets used in our study have been elaborated in the methods section. The relevant data can be obtained from the corresponding author upon reasonable request. Any additional information required to reanalyze the data reported in this paper is available from the Lead Contact upon request.

Declarations

Competing interests

The authors declare no competing interests.

Received: 16 January 2025 / Accepted: 18 February 2025
Published online: 26 February 2025

References

1. Shaw JE, Sicree RA, Zimmet PZ. Global estimates of the prevalence of diabetes for 2010 and 2030. Diabetes Res Clin Pract. 2010;87:4–14.
2. Li Y, Liu Y, Liu S, Gao M, Wang W, Chen K, et al. Diabetic vascular diseases: molecular mechanisms and therapeutic strategies. Signal Transduct Target Ther. 2023;8:152.
3. Augustin HG, Koh GY. Organotypic vasculature: from descriptive heterogeneity to functional pathophysiology. Science. 2017;357:eaal2379.
4. Marziano C, Genet G, Hirschi KK. Vascular endothelial cell specification in health and disease. Angiogenesis. 2021;24:213–36.
5. Gimbrone MA, García-Cardeña G. Endothelial cell dysfunction and the pathobiology of atherosclerosis. Circ Res. 2016;118:620–36.
6. Cong X, Kong W. Endothelial tight junctions and their regulatory signaling pathways in vascular homeostasis and disease. Cell Signal. 2020;66:109485.
7. Gaengel K, Genové G, Armulik A, Betsholtz C. Endothelial-mural cell signaling in vascular development and angiogenesis. Arterioscler Thromb Vasc Biol. 2009;29:630–8.
8. Wakabayashi T, Naito H. Cellular heterogeneity and stem cells of vascular endothelial cells in blood vessel formation and homeostasis: insights from single-cell RNA sequencing. Front Cell Dev Biol. 2023;11:1146399.
9. Paik DT, Tian L, Williams IM, Rhee S, Zhang H, Liu C, et al. Single-Cell RNA sequencing unveils unique transcriptomic signatures of Organ-Specific endothelial cells. Circulation. 2020;142:1848–62.
10. Kalucka J, de Rooij LPMH, Goveia J, Rohlenova K, Dumas SJ, Meta E, et al. Single-Cell transcriptome atlas of murine endothelial cells. Cell. 2020;180:764–e77920.
11. Song D, Yang D, Powell CA, Wang X. Cell–cell communication: old mystery and new opportunity. Cell Biol Toxicol. 2019;35:89–93.
12. Hao Y, Hao S, Andersen-Nissen E, Mauck WM, Zheng S, Butler A, et al. Integrated analysis of multimodal single-cell data. Cell. 2021;184:3573–e358729.
13. Germain P-L, Lun A, Garcia Meixide C, Macnair W, Robinson MD. Doublet identification in single-cell sequencing data using ScDblFinder. F1000Res. 2021;10:979.
14. Lun ATL, McCarthy DJ, Marioni JC. A step-by-step workflow for low-level analysis of single-cell RNA-seq data with bioconductor. F1000Res. 2016;5:2122.
15. Korsunsky I, Millard N, Fan J, Slowikowski K, Zhang F, Wei K, et al. Fast, sensitive and accurate integration of single-cell data with harmony. Nat Methods. 2019;16:1289–96.
16. Haber AL, Biton M, Rogel N, Herbst RH, Shekhar K, Smillie C, et al. A single-cell survey of the small intestinal epithelium. Nature. 2017;551:333–9.
17. Büttner M, Ostner J, Müller CL, Theis FJ, Schubert B. ScCODA is a bayesian model for compositional single-cell data analysis. Nat Commun. 2021;12:6876.
18. Jin S, Guerrero-Juarez CF, Zhang L, Chang I, Ramos R, Kuan C-H, et al. Inference and analysis of cell-cell communication using cellchat. Nat Commun. 2021;12:1088.
19. Raudvere U, Kolberg L, Kuzmin I, Arak T, Adler P, Peterson H, et al. G:Profiler: a web server for functional enrichment analysis and conversions of gene lists (2019 update). Nucleic Acids Res. 2019;47:W191–8.
20. Mootha VK, Lindgren CM, Eriksson K-F, Subramanian A, Sihag S, Lehar J, et al. PGC-1alpha-responsive genes involved in oxidative phosphorylation are coordinately downregulated in human diabetes. Nat Genet. 2003;34:267–73.
21. Subramanian A, Tamayo P, Mootha VK, Mukherjee S, Ebert BL, Gillette MA, et al. Gene set enrichment analysis: a knowledge-based approach for interpreting genome-wide expression profiles. Proc Natl Acad Sci U S A. 2005;102:15545–50.
22. Zhao Y, Jia X, Yang X, Bai X, Lu Y, Zhu L, et al. Deacetylation of Caveolin-1 by Sirt6 induces autophagy and retards high glucose-stimulated LDL transcytosis and atherosclerosis formation. Metabolism. 2022;131:155162.
23. Leng W, Ouyang X, Lei X, Wu M, Chen L, Wu Q, et al. The SGLT-2 inhibitor Dapagliflozin has a therapeutic effect on atherosclerosis in diabetic ApoE-/- mice. Mediators Inflamm. 2016;2016:6305735.
24. Xie J, Tato CM, Davis MM. How the immune system talks to itself: the varied role of synapses. Immunol Rev. 2013;251:65–79.
25. Sukumaran A, Coish JM, Yeung J, Muselius B, Gadjeva M, MacNeil AJ, et al. Decoding communication patterns of the innate immune system by quantitative proteomics. J Leukoc Biol. 2019;106:1221–32.

26. Uhlén M, Fagerberg L, Hallström BM, Lindskog C, Oksvold P, Mardinoglu A, et al. Proteomics. Tissue-based map of the human proteome. Science. 2015;347:1260419.
27. Ebefors K, Nyström J. New insights into crosstalk in the kidney. Curr Opin Nephrol Hypertens. 2017;26:143.
28. Freed JK, Gutterman DD. Communication is key: mechanisms of intercellular signaling in vasodilation. J Cardiovasc Pharmacol. 2017;69:264–72.
29. Welsh DG, Taylor MS. Cell-cell communication in the resistance vasculature: the past, present, and future. Microcirculation. 2012;19:377–8.
30. Ridker PM, Rane M. Interleukin-6 signaling and Anti-Interleukin-6 therapeutics in cardiovascular disease. Circ Res. 2021;128:1728–46.
31. Sakano Y, Sakano K, Hurrell BP, Helou DG, Shafiei-Jahani P, Kazemi MH, et al. Blocking CD226 regulates type 2 innate lymphoid cell effector function and alleviates airway hyperreactivity. J Allergy Clin Immunol. 2024;153:1406–e14226.
32. Yang C, Liu L, Lavayen BP, Larochelle J, Gunraj RE, Butler AA, et al. Therapeutic benefits of Adropin in aged mice after transient ischemic stroke via reduction of Blood-Brain barrier damage. Stroke. 2023;54:234–44.
33. McKerracher L, Rosen KM. MAG, Myelin and overcoming growth Inhibition in the CNS. Front Mol Neurosci. 2015;8:51.
34. Eelen G, Treps L, Li X, Carmeliet P. Basic and therapeutic aspects of angiogenesis updated. Circ Res. 2020;127:310–29.
35. Potente M, Gerhardt H, Carmeliet P. Basic and therapeutic aspects of angiogenesis. Cell. 2011;146:873–87.
36. Cochain C, Vafadarnejad E, Arampatzi P, Pelisek J, Winkels H, Ley K, et al. Single-Cell RNA-Seq reveals the transcriptional landscape and heterogeneity of aortic macrophages in murine atherosclerosis. Circ Res. 2018;122:1661–74.
37. Jaipersad AS, Lip GYH, Silverman S, Shantsila E. The role of monocytes in angiogenesis and atherosclerosis. J Am Coll Cardiol. 2014;63:1–11.
38. Naderi W, Schreiner D, King CG. T-cell-B-cell collaboration in the lung. Curr Opin Immunol. 2023;81:102284.
39. King DR, Sedovy MW, Eaton X, Dunaway LS, Good ME, Isakson BE, et al. Cell-To-Cell communication in the resistance vasculature. Compr Physiol. 2022;12:3833–67.
40. Hong K, Cope EL, DeLalio LJ, Marziano C, Isakson BE, Sonkusare SK. TRPV4 (Transient receptor potential vanilloid 4) Channel-Dependent negative feedback mechanism regulates Gq Protein-Coupled receptor-Induced vasoconstriction. Arterioscler Thromb Vasc Biol. 2018;38:542–54.
41. Biwer LA, Good ME, Hong K, Patel RK, Agrawal N, Looft-Wilson R, et al. Non-Endoplasmic Reticulum-Based Calr (Calreticulin) can coordinate heterocellular calcium signaling and vascular function. Arterioscler Thromb Vasc Biol. 2018;38:120–30.
42. Li X, Sun X, Carmeliet P. Hallmarks of endothelial cell metabolism in health and disease. Cell Metab. 2019;30:414–33.
43. Rangaswami J, Bhalla V, Blair JE, Chang TI, Costa S, Lentine KL, et al. Cardiorenal syndrome: classification, pathophysiology, diagnosis, and treatment strategies: A scientific statement from the American heart association. Circulation. 2019;139:e840–78.
44. Méndez Fernández AB, Vergara Arana A, Olivella San Emeterio A, Azancot Rivero MA, Soriano Colome T, Soler Romeo MJ. Cardiorenal syndrome and diabetes: an evil pairing. Front Cardiovasc Med. 2023;10:1185707.
45. Li W, Lou X, Zha Y, Qin Y, Zha J, Hong L et al. Single-cell RNA-seq of heart reveals intercellular communication drivers of myocardial fibrosis in diabetic cardiomyopathy. eLife 2023;12:e80479.
46. Tuleta I, Frangogiannis NG. Diabetic fibrosis. Biochim Biophys Acta Mol Basis Dis. 2021;1867:166044.
47. Li J, Liu H, Srivastava SP, Hu Q, Gao R, Li S, et al. Endothelial FGFR1 (Fibroblast growth factor receptor 1) deficiency contributes differential fibrogenic effects in kidney and heart of diabetic mice. Hypertension. 2020;76:1935–44.
48. Amrute JM, Luo X, Penna V, Yang S, Yamawaki T, Hayat S, et al. Targeting immune–fibroblast cell communication in heart failure. Nature. 2024;635:423–33.
49. Tuleta I, Frangogiannis NG. Fibrosis of the diabetic heart: clinical significance, molecular mechanisms, and therapeutic opportunities. Adv Drug Deliv Rev. 2021;176:113904.
50. Chen D, Shao M, Song Y, Ren G, Guo F, Fan X, et al. Single-cell RNA-seq with Spatial transcriptomics to create an atlas of human diabetic kidney disease. FASEB J. 2023;37:e22938.
51. Maisons V, Halimi J-M, Fauchier G, de Fréminville J-B, Goin N, Gueguen J, et al. Type 2 diabetes and cardiorenal syndromes. A nationwide French hospital cohort study. Diabetes Metab. 2023;49:101441.
52. Fitchett D, Inzucchi SE, Cannon CP, McGuire DK, Scirica BM, Johansen OE, et al. Empagliflozin reduced mortality and hospitalization for heart failure across the spectrum of cardiovascular risk in the EMPA-REG OUTCOME trial. Circulation. 2019;139:1384–95.
53. Heerspink HJL, Oshima M, Zhang H, Li J, Agarwal R, Capuano G, et al. Canagliflozin and Kidney-Related adverse events in type 2 diabetes and CKD: findings from the randomized CREDENCE trial. Am J Kidney Dis. 2022;79:244–e2561.
54. Wheeler DC, Stefánsson BV, Jongs N, Chertow GM, Greene T, Hou FF, et al. Effects of Dapagliflozin on major adverse kidney and cardiovascular events in patients with diabetic and non-diabetic chronic kidney disease: a prespecified analysis from the DAPA-CKD trial. Lancet Diabetes Endocrinol. 2021;9:22–31.
55. Li J, Wang Q, Chai W, Chen M-H, Liu Z, Shi W. Hyperglycemia in Apolipoprotein E-deficient mouse strains with different atherosclerosis susceptibility. Cardiovasc Diabetol. 2011;10:117.
56. Wu J, Sun Z, Yang S, Fu J, Fan Y, Wang N, et al. Kidney single-cell transcriptome profile reveals distinct response of proximal tubule cells to SGLT2i and ARB treatment in diabetic mice. Mol Ther. 2022;30:1741–53.
57. Wu H, Gonzalez Villalobos R, Yao X, Reilly D, Chen T, Rankin M, et al. Mapping the single-cell transcriptomic response of murine diabetic kidney disease to therapies. Cell Metab. 2022;34:1064–e10786.
58. Hu Y, Zhao Y, Li P, Lu H, Li H, Ge J. Hypoxia and panvascular diseases: exploring the role of hypoxia-inducible factors in vascular smooth muscle cells under panvascular pathologies. Sci Bull. 2023;68:1954–74.
59. Xu S, Ilyas I, Little PJ, Li H, Kamato D, Zheng X, et al. Endothelial dysfunction in atherosclerotic cardiovascular diseases and beyond: from mechanism to pharmacotherapies. Pharmacol Rev. 2021;73:924–67.
60. Efremova M, Vento-Tormo M, Teichmann SA, Vento-Tormo R. CellPhoneDB: inferring cell-cell communication from combined expression of multi-subunit ligand-receptor complexes. Nat Protoc. 2020;15:1484–506.
61. Noël F, Massenet-Regad L, Carmi-Levy I, Cappuccio A, Grandclaudon M, Trichot C, et al. Dissection of intercellular communication using the transcriptome-based framework ICELLNET. Nat Commun. 2021;12:1089.
62. Cohen M, Giladi A, Gorki A-D, Solodkin DG, Zada M, Hladik A, et al. Lung Single-Cell signaling interaction map reveals basophil role in macrophage imprinting. Cell. 2018;175:1031–e104418.
63. Ximerakis M, Lipnick SL, Innes BT, Simmons SK, Adiconis X, Dionne D, et al. Single-cell transcriptomic profiling of the aging mouse brain. Nat Neurosci. 2019;22:1696–708.
64. Wang L, Yu P, Zhou B, Song J, Li Z, Zhang M, et al. Single-cell reconstruction of the adult human heart during heart failure and recovery reveals the cellular landscape underlying cardiac function. Nat Cell Biol. 2020;22:108–19.
65. Di X, Gao X, Peng L, Ai J, Jin X, Qi S, et al. Cellular mechanotransduction in health and diseases: from molecular mechanism to therapeutic targets. Signal Transduct Target Ther. 2023;8:282.
66. Rieckmann JC, Geiger R, Hornburg D, Wolf T, Kveler K, Jarrossay D, et al. Social network architecture of human immune cells unveiled by quantitative proteomics. Nat Immunol. 2017;18:583–93.
67. Stary HC. Natural history and histological classification of atherosclerotic lesions: an update. Arterioscler Thromb Vasc Biol. 2000;20:1177–8.
68. Eelen G, de Zeeuw P, Simons M, Carmeliet P. Endothelial cell metabolism in normal and diseased vasculature. Circ Res. 2015;116:1231–44.
69. Barnett SN, Cujba A-M, Yang L, Maceiras AR, Li S, Kedlian VR, et al. An organotypic atlas of human vascular cells. Nat Med. 2024;30:3468–81.
70. Billing AM, Kim YC, Gullaksen S, Schrage B, Raabe J, Hutzfeldt A, et al. Metabolic communication by SGLT2 Inhibition. Circulation. 2024;149:860–84.
71. Clyne AM. Endothelial response to glucose: dysfunction, metabolism, and transport. Biochem Soc Trans. 2021;49:313–25.
72. van Dijk CGM, Oosterhuis NR, Xu YJ, Brandt M, Paulus WJ, van Heerebeek L, et al. Distinct endothelial cell responses in the heart and kidney microvasculature characterize the progression of heart failure with preserved ejection fraction in the obese ZSF1 rat with cardiorenal metabolic syndrome. Circ Heart Fail. 2016;9:e002760.
73. Gomez-Puerto MC, Iyengar PV, García de Vinuesa A, Ten Dijke P, Sanchez-Duffhues G. Bone morphogenetic protein receptor signal transduction in human disease. J Pathol. 2019;247:9–20.
74. Chen Y, Ma B, Wang X, Zha X, Sheng C, Yang P, et al. Potential functions of the BMP family in bone, obesity, and glucose metabolism. J Diabetes Res. 2021;2021:6707464.

75. Sun L, Yu J, Qi S, Hao Y, Liu Y, Li Z. Bone morphogenetic protein-10 induces cardiomyocyte proliferation and improves cardiac function after myocardial infarction. J Cell Biochem. 2014;115:1868–76.
76. Dekker E, Triñanes J, Muñoz Garcia A, de Graaf N, de Koning E, Carlotti F. Enhanced BMP signaling alters human β-cell identity and function. Adv Biol. 2025;9:2400470.
77. Zhang M, Sara JD, Wang F, Liu L-P, Su L-X, Zhe J, et al. Increased plasma BMP-2 levels are associated with atherosclerosis burden and coronary calcification in type 2 diabetic patients. Cardiovasc Diabetol. 2015;14:64.
78. Hussein KA, Choksi K, Akeel S, Ahmad S, Megyerdi S, El-Sherbiny M, et al. Bone morphogenetic protein 2: a potential new player in the pathogenesis of diabetic retinopathy. Exp Eye Res. 2014;125:79–88.
79. Fujita Y, Tominaga T, Abe H, Kangawa Y, Fukushima N, Ueda O, et al. An adjustment in BMP4 function represents a treatment for diabetic nephropathy and podocyte injury. Sci Rep. 2018;8:13011.

Publisher's note

Springer Nature remains neutral with regard to jurisdictional claims in published maps and institutional affiliations.